# INTERNAL VISCOELASTIC LOADING IN CAT PAPILLARY MUSCLE

YU-LAM CHIU, EDMUND W. BALLOU, AND LINCOLN E. FORD
*Department of Medicine, University of Chicago, Chicago, Illinois 60637*

ABSTRACT The passive mechanical properties of myocardium were defined by measuring force responses to rapid length ramps applied to unstimulated cat papillary muscles. The immediate force changes following these ramps recovered partially to their initial value, suggesting a series combination of viscous element and spring. Because the stretched muscle can bear force at rest, the viscous element must be in parallel with an additional spring. The instantaneous extension-force curves measured at different lengths were nonlinear, and could be made to superimpose by a simple horizontal shift. This finding suggests that the same spring was being measured at each length, and that this spring was in series with both the viscous element and its parallel spring (Voigt configuration), so that the parallel spring is held nearly rigid by the viscous element during rapid steps. The series spring in the passive muscle could account for most of the series elastic recoil in the active muscle, suggesting that the same spring is in series with both the contractile elements and the viscous element. It is postulated that the viscous element might be coupled to the contractile elements by a compliance, so that the load imposed on the contractile elements by the passive structures is viscoelastic rather than purely viscous. Such a viscoelastic load would give the muscle a length-independent, early diastolic restoring force. The possibility is discussed that the length-independent restoring force would allow some of the energy liberated during active shortening to be stored and released during relaxation.

## INTRODUCTION

Since introduced by Abbott and Mommaerts in 1959, the papillary muscle has been widely used to study the physiological properties of myocardium. Mechanical studies of the preparation are complicated by a stiff parallel compliance over a portion of its functioning range and a relatively large series compliance, most of which resides in the crushed tissue where the muscle is gripped. Correction of the measured muscle force and velocity to obtain contractile element force and velocity depends on the arrangement of parallel and series elasticities assumed for the muscle (Hefner and Bowen, 1967; Pollack, 1970). In an effort to define the arrangement, we have made a servo system capable of performing critically damped force or length steps that are complete within 1–2 ms. When such steps are applied to papillary muscle, the immediate responses of both the active and passive muscle are dominated by the passive viscoelastic properties of the preparation. Analysis of these responses requires an accurate description of the compliance of the crushed tissue at the ends of the muscle where the preparation is gripped, and so we have devoted a substantial effort to defining the mechanical properties of this artifactually produced compliance. The present paper describes the passive properties of the papillary muscle and their possible physiological role. The following paper describes their effect on the mechanical capabilities of the activated preparation.

## METHODS

### Preparation

Adult cats were anesthetized with an intraperitoneal injection of 125–250 mg sodium pentobarbital and the hearts excised. Right ventricular papillary muscles were selected to have a free length between the attachments of at least 5 mm, and a diameter <1.1 mm. This selection yielded muscles with a mean cross-sectional area of <1 $mm^2$. Muscles were rejected immediately if the ratio of passive force to actively developed force >0.2 at the length where maximum active force was developed ($L_{max}$). This ratio was <0.15 in all muscles finally studied. During dissection, care was taken to keep the muscle well irrigated with oxygenated physiologic salt solution. After dissection and mounting, the muscles were maintained at 26°–28°C and stimulated regularly every 4 s, approximately the optimum frequency for both force development and data collection. To standardize conditions, the muscles were stimulated to contract isometrically for at least seven beats between each isotonic contraction. When passive properties were studied, the eighth stimulus was inhibited and the steps were applied at the same time in the stimulus cycle as when active contractions were studied, so as to relate the passive properties as closely as possible to the active responses. The muscles contracted reproducibly for 16–24 h, and during that time, 1,000–2,000 isotonic contractions were studied.

*Muscle Attachments.* Both ends of the muscle were gripped with 25-$\mu$m thick platinum foil clips, larger but similar in shape to those described by Ford et al. (1977). A silk suture was tied around the *chordae tendineae* to prevent the tendons from slipping out of the clips. A sufficient amount of ventricular tissue was left at the other end to prevent slippage. The size of the clips was selected in each experiment to fit the muscle. In general, the clip at the tendon end was ~0.5 mm wide when closed and the other clip was three to four times wider. The preparation

was mounted on the apparatus by passing holes in the clips over hooks (125-$\mu$m thick) attached to the motor and transducer. The lighter clip at the tendon end was always placed over the transducer hook.

*Fiber Measurement and Photography.* Muscle length and diameter were measured with a reticle in the eyepiece of a dissecting microscope set at a total magnification of 10× (Nikon, Inc., Instrument Div., Garden City, NJ, model SM-5). In several fibers, carbon granules were placed on the surface of the muscle and their movement was used to assess stretching of the compliant ends of the muscle as well as shearing within the muscle. To resolve the time course of this movement, cine photographs of the muscle were taken with a Bolex (Yverdon, Switzerland) 16-mm camera focused down one eyepiece of the microscope and run at 64 frames per second.

At the end of the experiment, the muscle was cut out of its attachments and weighed. The mean cross-sectional area was determined as weight ÷ ($1.05 \times L_{max}$), 1.05 gm/cm$^3$ being taken as the density of muscle.

*Stimuli.* Stimuli were 1-ms duration square pulses passed through 3 × 10-mm bright platinum electrodes held against the sides of the trough, parallel to the muscle. A 5-KΩ potentiometer in series with the electrodes and a 12 V source was adjusted to give pulses slightly above threshold.

## Apparatus

*Servo Motor and Force Transducer.* The rotating coil motor was identical to that described by Ford et al. (1977) except that it had a slightly shorter extension arm, 30 instead of 41 mm. A cantelevered piezoelectric force transducer (Chiu et al., 1978) with a 4-mm free length of piezoelectric element and a 6-mm glass extension was used. The transducer had a compliance of 2.5 $\mu$m/g and a natural resonance of 8 KHz, which was sufficiently high that no effort was made to damp it. The humidity in the air above the trough tended to short circuit the capacitative electrodes in the sensing element. To minimize this current leak, dry air was blown over the transducer throughout the experiment. When used in this manner, the output of the transducer decayed to the base line with a time constant >25 s following a force step. This decay introduced a maximum error of 2% in the absolute value of force during any contraction, and an error of <1% in the force during the period of recording following a length perturbation. This transducer was used in spite of its inability to produce a steady DC signal because of its high resonant frequency, which is required when the transducer is used to produce force steps in a servo loop.

## Servo System

The servo system was very similar to that described by Ford et al. (1977) except that it did not include a sarcomere-length sensor and it did include a delayed-gain amplifier in parallel with the main servo amplifier. This additional amplifier increased the steady-state stiffness of the system without causing the instability that would be created by a similarly high instantaneous loop gain (Gordon et al., 1966, p. 152). The position of the motor arm could be controlled either by a signal from the motor's internal position sensor (position control) or by the force signal (force control). Switching between the two types of control was accomplished by a diode switching network identical to that used by Ford et al. (1977). In studying activated muscle, force was allowed to develop isometrically with the system in position control, and then the system was switched into force control, with force held constant at a fraction of the isometric level immediately before the step while the muscle shortened. In studying the passive muscle, single steps were made from one length to another, with the system only in position control.

To eliminate base line drift from the force signal and establish a reproducible force reference, the output of the force amplifier was passed through a "track and hold" circuit (Nakajima et al., 1976). This device substracted the input from itself, holding the output to zero until a pulse was applied at the time the muscle was stimulated. With this pulse present, the output began at zero and tracked the input signal. The zero reference is therefore the level of force immediately before stimulation, irrespective of the rest force. The absolute level of rest force was determined by applying sufficiently large releases to make the resting muscle go slack, and measuring the drop in force. Slackness was determined by showing that an increase in step size produced no further drop in force.

*Timing.* The timing of all events, including muscle stimulation, triggering recording devices, setting camera exposures, and switching of servo system was controlled by digital logic modules made by BRS/LVE Inc. of Beltsville, MD.

## Recording

Four types of recordings were made: 35-mm film records of oscilloscope tracings used as permanent, hard records; strip chart recording of force and length, used to assess muscle performance during the experiments; digital records made by computer and stored on floppy disks; and transient recordings obtained with a Physical Data, Inc. (Beaverton, OR) 513A recorder and displayed on a second oscilloscope immediately after each step. These last records were used to judge the speed and quality of the steps, and when necessary, to adjust parameters in the servo-loop.

*Computer Recording.* Analog-to-digital conversion and data storage was performed by a PDP 11/10 computer (Digital Equipment Corporation, Marlboro, MA) with an AR11 input-output device. Typically, 250 10-bit words were sampled sequentially in each of four channels, usually at intervals of 200 $\mu$s/channel, recording 10 samples as a base line before the contraction began and 240 samples starting 10 sample intervals before the step. In some experiments, data were taken in at 1/4 the above rate, and in all experiments some records were also taken of force and length at 1/20 the normal speed to record entire contractions each time the length was changed. The four data channels were force, length, and two channels of high gain length used to determine velocity. Force and length signals were amplified and offset so as to nearly fill the input voltage range of the computer (±2.5 V) when the largest changes in the experiments were encountered. The gain settings of these amplifiers were rarely changed during an experiment.

*Velocity Recording.* Velocity was determined by digitally differentiating the length signal. To provide a reasonable degree of velocity resolution, the length trace was amplified and fed into two separate channels with one offset from the other by ~90% of the input voltage range. The gain of this amplified length trace was adjusted repeatedly for different steps so that, as a minimum, it nearly saturated one input channel, and as a maximum, never quite fully saturated both inputs. The amplifier gain could be increased manually by successive factors of two.

*Digital Data Storage.* Although data were taken into the computer with 10 bit analog-to-digital converters, they were stored in eight-bit, byte form for economy. Because velocity never exceeded 255, only the eight least significant bits needed to be stored. The force and low gain length data were packed into byte form by subtracting the minimum value in the trace and successively dividing by two, until the maximum was <256. This procedure provided a minimum resolution of 1/128 over an eightfold range of data values.

*Data display.* Oscilloscope displays used in the following figures are from digital data stored in the computer and later reconverted to analog signals. In some displays, the velocity data has been smoothed

and amplified using the formula (Kendall, 1976, p. 31).

$$X_{is} = \frac{1}{21}[7X_i + 6(X_{i-1} + X_{i+1}) + 3(X_{i-2} + X_{i+2}) - 2(X_{i-3} + X_{i+3})]. \quad (1)$$

This provides a digital filter at ~1 KHz. Calculations were always made on unfiltered data or on data averaged over a specific period of time, as described in the text.

## RESULTS

Results were based on data from seven papillary muscles having the characteristics shown in Table I. Rest tension averaged 6.1 ± 2.3 SD mN/mm$^2$ at $L_{max}$ (the length where maximum active force was developed) and decreased to 37% ($1/e$) at a length between 0.9 and 0.95 $L_{max}$. The properties of the passive (unstimulated) muscle were defined by applying length ramps completed within 2–10 ms and studying the resultant force responses. The properties of the active (stimulated) muscle were defined using steps from an isometric length to an isotonic force and both length and velocities were studied. These steps were complete within 1–2 ms.

The data obtained were analyzed with the goal of constructing a conceptual model to simulate the papillary muscle. First, the basic three-component model was identified, and, as fine points of the data were analyzed, additional refinements of this basic model were made. Also, comparisons between the active and passive muscle were made to study the relationship between the contractile elements and the passive elements.

### Length Steps Applied to the Passive Muscle

*Extension-force characteristics.* When a rapid length step (either lengthening or shortening) was applied to the resting muscle, the force change immediately following the step was greater than that measured in the steady state. A response to a shortening ramp is shown in Fig. 1 (*inset*); a lengthening ramp would produce similar but opposite responses. The force change has four distinct stages (Fig. 1, *inset*): At the beginning of the ramp, there is a small, nearly instantaneous drop in force (stage 1). This is followed (stage 2) by a smooth continuous decrease in force for the duration of length change. At the end of the ramp, there is a small, rapid increase in force (stage 3), similar in size and time course to the force drop at the beginning. Finally, there is the slow, gradual phase of force recovery towards the steady state after length change has been completed (stage 4). (These stages are not at all related to the four "phases" used in the following paper to describe the transients of the active muscle).

The "immediate" force responses (Fig. 1: O, —) were measured as the force immediately following the ramp, after the nearly instantaneous small jump in force (stage 3) had ended, but before the start of the slow recovery towards the steady state. Releases were made from three different initial lengths. The steady-state forces (×, ---) were measured after the muscle had remained at each length for many minutes. The muscle shown was chosen because it had a measurable rest force over a comparatively long range of length.

*Arrangement of Elasticity and Viscosity.* The slow force recovery demonstrated above requires a series combination of an elastic element (spring), and a viscous element (dashpot). Because the muscle bears force at rest and because a simple dashpot is freely extensible in the steady state, the viscous element must be in parallel with another spring. This spring (labeled $p$ in Fig. 2) could either be added in series (Voigt configuration, Fig. 2 *A*) or in parallel (Maxwell configuration, Fig. 2 *B*) with the first spring (spring $s$). The immediate extension-force curves

TABLE I
PAPILLARY MUSCLES

| Muscle number | Length | Weight | Cross section | Developed tension | Rest tension |
|---|---|---|---|---|---|
| | *mm* | *mg* | *mm$^2$* | *nN/mm$^2$* | *mN/mm$^2$* |
| 1 | 5.0 | 5.0 | 0.95 | 60 | 5.4 |
| 2 | 6.0 | 5.8 | 0.92 | 37 | 6.8 |
| 3 | 6.4 | 6.5 | 0.97 | 37 | 2.9 |
| 4 | 6.0 | 6.3 | 1.00 | 90 | 5.5 |
| 5 | 5.4 | 2.0 | 0.35 | 85 | 6.6 |
| 6 | 6.0 | 1.2 | 0.19 | 60 | 5.0 |
| 7 | 5.3 | 2.8 | 0.50 | 68 | 10.4 |
| mean | 5.7 | 4.2 | 0.70 | 62 | 6.1 |

All measurements made at $L_{max}$.

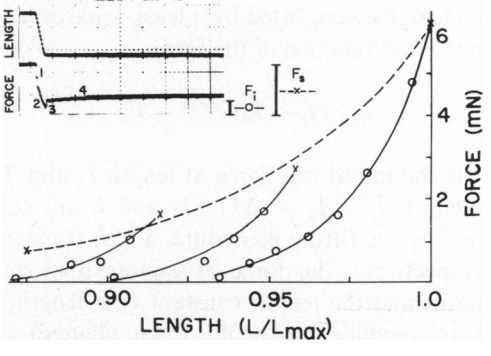


FIGURE 1 Extension-force characteristics of passive muscle. The records in the *inset* show the way in which the measurements are made. The four stages, labeled 1–4, are described in the text. $F_i$, the immediate force response is measured ~1 ms after the ramp ended. $F_s$, the steady-state force is measured by applying sufficiently large release to make the muscle go slack, and measuring the drop in force. Solid curves and O represent immediate force levels following a 2 ms ramp starting from three different initial lengths (×). Interrupted curve and ×, the steady-state force in the muscle after it had remained at each length for many minutes. The three solid curves represent the same exponential function shifted horizontally. Muscle No. 2, same muscle used in Figs. 4, 5, 6, and 8.

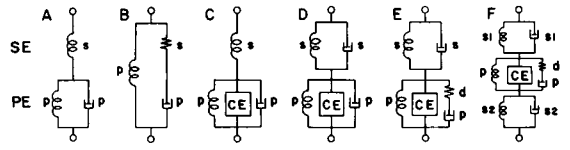


FIGURE 2 Arrangements of springs and viscous elements. Springs that would remain extended during shortening are represented as coils, to distinguish them from those that would become compressed, drawn as folding structures. Arguments are presented in the text to show that *A*, the Voigt configuration, is a more likely representation of the muscle than *B*, the Maxwell configuration. *C–F* show additions made to *A*. *C* shows how the contractile elements of the stimulated muscle, CE, are related to the passive components. The designations s and p stand for series and parallel, respectively, because of the relationship of the different components to the contractile elements. Further evidence suggests that the series spring is lightly damped, hence the addition of dashpot s in D. An argument is made that the parallel viscosity is actually viscoelastic, and so spring d has been added in *E*. Finally, the possibility is considered that the damped series spring is two separate springs, one at each end of the muscle, and that ends may have different amounts of damping. This arrangement is shown in *F*.

obtained at different lengths shown above were found to be nearly identical in that they could be made to superimpose by a simple horizontal shift. This suggests that the same spring was being measured at each length. The Voigt model will produce this response because the viscous element is nearly rigid during rapid length changes and only the spring in series with it (spring s) changes length.

The extent to which the immediate extension-force curves obtained at different lengths could be superimposed was assessed quantitatively by comparing curves obtained at two lengths in the seven muscles. The longer length was $L_{max}$, and the shorter length was such that the rest force was 34–43% of that at $L_{max}$. In two muscles, both stretches and releases were performed, in the remaining five, only releases were studied. The extension-force curves obtained at the two lengths were fitted by a least-squares technique to an exponential function of the form

$$T = (T_i + T_o)\, e^{\Delta L/k} - T_o \qquad (2)$$

where $T_i$ is the initial rest force at length $L_i$ and $T$ is the force at length $L = L_i + \Delta L$. $T_o$ and $k$ are constants determined by the fitting procedure. These constants represent, respectively, the force asymptote approached at short lengths and the length constant (the length change required to produce an $e$-fold force change). If two different curves have the same $T_o$ and $k$ they are superimposable. When the values of the $T_o$ fitted to the curve for the longer length was compared to the $T_o$ of the shorter length they were found to be nearly the same. Paired $t$-test on the differences between the two groups of $T_o$ showed that they were insignificant, with $p > 0.9$. The average values of $T_o$ was 0.01 times the rest force at $L_{max}$. Paired $t$-tests of the differences of the $k$ values also showed that they were insignificant ($p > 0.9$). $k$ averaged 0.2 $L_{max}$ $\pm 0.002$ SD at $L_{max}$ and 1.03 times this value at the shorter length.[1]

*Defining Parameters of the Model.* The parameters of the springs in the Voigt model are determined as follows: The immediate extension-force curves were assumed to be determined by the series spring (s) alone, so that constants used to fit the instantaneous curves were used to describe it. The steady-state compliance of the overall model in Fig. 2 *A* is the sum of the compliances ($dL/dT$ = 1/stiffness) of the two springs in series. The extension-force characteristics of the parallel spring (p) alone was therefore determined by subtracting the compliance of the immediate curves from the steady-state compliance. In terms of Fig. 1, this was done by subtracting, horizontally at each level of force, the length of the immediate curve from the length of the steady-state curve.

The stiffness of the two springs thus specifies both the immediate and the steady-state forces for all length changes. The time course of approach to the steady-state is determined by the viscous element. For simplicity, it was assumed to be a simple dashpot and was described by a constant, $Q$ such that

$$Q = T \div dL/dt \qquad (3)$$

where $dL/dt$ is the rate of length change of the dashpot and $T$ the force across it. The value of $Q$ was chosen such that the calculated response most closely resembled the data.

The force responses for the model were calculated by a numerical Runge-Kutta (Carnahan et al., 1969, p. 361) solutions of Eqs. 2 and 3 (see Appendix), using the digitized length record as a driving function. The value of

[1]The observation that the average force asymptote, $T_o$, was very nearly zero implies that the immediate stiffness, $dT/dL$, was approximately proportional to $T_i$ and approached zero at short lengths. This finding argues strongly against the Maxwell configuration (Fig. 2 *B*). In this configuration, the spring s in series with the viscosity becomes compressed during shortening steps, and for this reason it is drawn as a folding structure in Fig. 2 *B*. Such an element is likely to become more stiff as it is compressed, while the data would require it to become less stiff, making the Maxwell model qualitatively unlikely. A quantitative argument against the Maxwell configuration is based on two considerations: (*a*) that the two springs in this configuration are in parallel, so that their stiffness is additive, and (*b*) that the viscous elements are fully extensible in the steady-state. Because of the extensibility, the series spring in the Maxwell configuration returns to its rest position and length steps applied to the overall muscle at any length are always applied to the compressive spring starting at the same, unstressed length. The instantaneous stiffness, therefore, should be the sum of the steady-state stiffness, which is dependent on muscle length, and the stiffness of the compressive spring, which is independent of muscle length. When steps are made from progressively shorter initial lengths, where the steady-state stiffness approaches zero, the instantaneous stiffness should approach the constant value of the compressive spring and be independent of the initial length or tension, instead of being proportional to initial force and dependent on initial length, as found in these experiments.

the damping factor, $Q$, in Eq. 3 was adjusted to match the rate of partial force recovery following a length step. The constants $k$ and $T_0$ in Eq. 2 used to describe the series spring were also adjusted slightly to account for the force recovery during the step. An example of a family of steps including two stretches and two releases, matched in this way, is shown in Fig. 3 *A*. The upper four pairs of traces are the paired calculated and observed force responses. The middle four traces are the differences between the paired responses. The bottom four traces are the superposed length records. As shown, the model fits the data moderately well.

The damping constants for the parallel viscosity determined by this procedure averaged 45 ± 10 SD (mN·s/mm$^2$·$L_{max}$) in six muscles.

Fig. 3 *A* shows that partial force recovery is more rapid following a large stretch than a large release. This difference is due to the exponential nature of the springs, which are stiffer at higher forces. The nonlinearity of the springs does not permit the use of a single time constant to describe recovery speed.

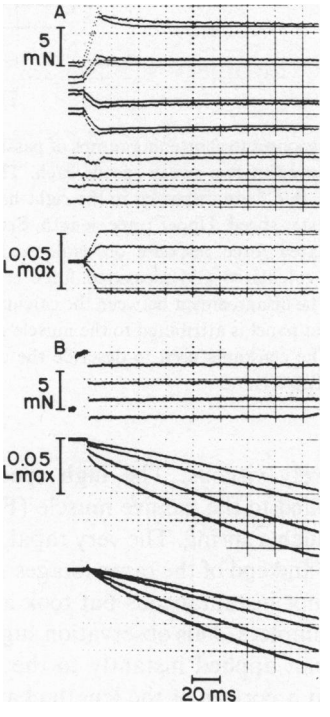


FIGURE 3 Time course of responses to force and length steps. *A*, force responses to four length steps, two releases and two stretches, applied to the unstimulated muscle. Upper panel, four pairs of force responses. The noisier trace in each pair is the data and the quieter trace is the calculated response, as described in the text. Middle panel, difference between calculated and observed force at the same amplification. Lower panel, the four length records superimposed. The rapid force changes at the beginning and end of the length ramp, stages 1 and 3, are not as large as those in the *inset* of Fig. 1 because the ramps are five times slower. They are clearly seen in the difference records, however, as would be expected since the calculated responses do not yet attempt to account for these very rapid changes. *B*, length responses to four force steps applied to activated muscle during four different twitches. Upper panel, superimposed force records. First 4 ms, opposite bottom of the calibration bar, are base line force recorded before stimulation. The recording is not continuous, but waits until 8 ms before the force step, so that the next 8 ms are isometric force recorded immediately before release. Remainder of trace is isotonic force following the step. The isotonic force in the largest step goes below the base line rest force. Middle panel, superimposed length records. Lower panel, length minus calculated series elastic recoil. Muscle No. 5, same muscle used in Fig. 8.

## Force Steps Applied to the Active Muscle

To study the relationship of the contractile element to the passive structures, isotonic force steps were applied to isometrically contracting muscles. Fig. 3 *B* shows the shortening responses to four steps applied to the active muscle. These responses include a period of early rapid shortening attributed to shortening of the series spring (series elastic recoil) followed by a slower, isotonic shortening. The steps were made at $L_{max}$ early in the twitch, when developed force was ~25% of its maximum, and did not exceed the greatest force achieved during stretches of the passive muscle. In addition, the isotonic force following the largest force step was well below the initial force base line, so that the ranges of force in the active and passive muscle were directly comparable. The parameters used to describe the series spring in the passive muscle (the calculated force response in the upper panel of Fig. 3 *A*) were also used to calculate the series elastic recoil in the active muscle. When this calculated amount of shortening was subtracted from the length data, isotonic shortening appears to begin without a rapid initial step from the isometric base line (lowest panel in Fig. 3 *B*), showing that the series springs in the active and passive muscles were similiar. This similarity was evaluated further by comparing the calculated and measured shortening in 20 force steps in each of 7 muscles. 10 steps to different isotonic loads were made early in the contraction and 10 steps were made at the time of peak force. In the 140 steps examined, the calculated shortening averaged 0.98 ± 0.11 SD of the measured value. This similarity between the series spring in the active and passive muscle, suggests that the same spring is being measured under both conditions, i.e., that the spring in series with the passive viscosity is also in series with the contractile elements (Fig. 2 *C*). This conclusion is reinforced by the consideration that the heavily damped spring (spring $p$) seen in the passive muscle is unlikely to be in series with the contractile elements. If it were, very little rapid series elastic recoil would be observed. The proposed arrangement places the viscous element in parallel with the contractile element, as shown in Fig. 2 *C*. Because of these relationships to the contractile elements, the elements in the lower half of Fig. 2 are labeled PE, for parallel elements, and those in the upper half are labeled SE for series elements, with the individual components labeled p and s, respectively.

## Series Elastic Damping

The length responses to steps made early in the contraction, as in Fig. 3 *B*, were easier to analyze than those made later in the contraction. The later steps resulted in a length trace that was considerably rounded, so that it was difficult to determine where the series elastic recoil ended and the isotonic shortening began (Fig. 4). Two factors contributed to this rounding; (*a*) the rate of isotonic shortening declined progressively throughout the trace and (*b*) the series elastic recoil persisted for several milliseconds after the step ended, with no discontinuity at the end of the step. Both of these features were greatest in steps to the lowest loads, and are more evident in the velocity traces (lower most trace in Fig. 4). The persistence of the recoil is also better seen when the same records are displayed at a faster sweep speed (Fig. 4 *B*).

The persistence of the series elastic recoil can be attributed to very light damping of the series spring (Fig. 2 *D*). The damping constant in this case was calculated to be 200–300 times less than that of the parallel viscosity, so that the recoil persisted for only a brief time, <3–4 ms beyond the end of the step. Additional evidence for series damping could be found in high speed records of force responses during rapid length ramps applied to the passive muscle. There was a rapid drop in force at the onset of a shortening step and a rapid rise at the end. Small changes of this sort are seen in Fig. 3 *A*, but are more obvious in Fig. 5, where the length changes are five times faster.

## Load on the Contractile Element

The model in Fig. 2 *D* has the contractile element directly in parallel with a dashpot. This arrangement imposes a substantial load on the rapidly shortening contractile elements, which would be very inefficient. For reasons described in the Discussion, a likely explanation is that the viscous element is in series with an additional spring, so that the load on the contractile elements is viscoelastic,

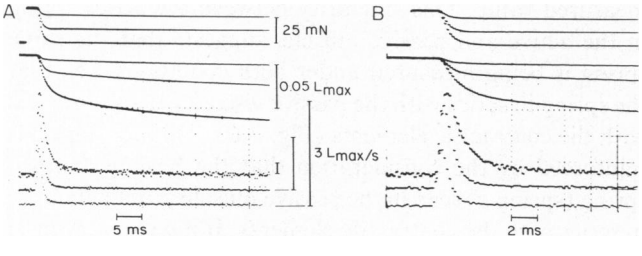


FIGURE 4 Force steps applied to active muscle. Three sizes of step displayed at two sweep speeds. The same records are displayed in both *A* and *B*. In *B* the records are shown at 2½ times faster sweep speed. Upper trace, force with the base line shown as first 1.5 ms. Middle trace, length. Lower trace, velocity. Note that the gain of velocity traces is increased in the steps to higher force and that the uppermost velocity trace corresponds to the step to the lowest loads. The high velocity associated with the step lasts longer than the force step, and this prolongation is more marked in steps to lower forces.

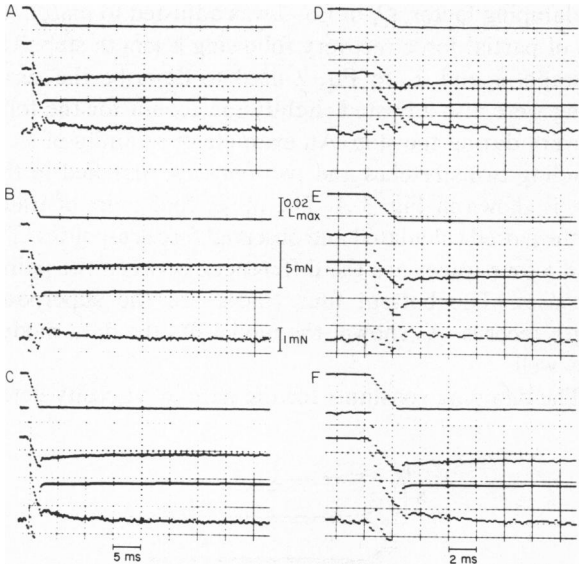


FIGURE 5 Force responses to shortening ramps of passive muscle. Three sizes of ramp, displayed at two sweep speeds each. The records in the left-hand panels (*A, B, C*) are displayed in the right-hand panels (*D, E, F*) at a 2½ times faster speed. Upper trace, length. Second trace, force. Third trace, calculated force response on same scale. Fourth trace, difference between calculated and measured force response, on 2 1/2 times larger scale. The disagreement between the calculated response and the data in the lowest panel is attributed to the muscle going slack at the end of the ramp. The constants used to describe the component in the model are listed in Table II.

rather than purely viscous. The high speed records of length steps applied to the passive muscle (Fig. 5) suggest the presence of such a spring. The very rapid force changes at the beginning and end of the ramp (stages 1 and 3 in Fig. 1 [*inset*]) were not instantaneous but took a fraction of a millisecond to complete. This observation suggests that the length ramp is not applied instantly to the series viscous element, but that a portion of the length change is applied to a spring in series with it. For the purposes of analysis, this additional spring (spring d) was added to the model in Fig. 2 *D* in parallel with the spring p (Fig. 2 *E*). A spring in this position operates in compression during shortening and so is drawn as a folding structure. It also, in a way, decouples the purely viscous load from the contractile elements so it is called the "decoupling" spring here. For simplicity it was assumed to have linear force-extension characteristics defined by a constant, $h$, such that

$$h = T/\Delta L \qquad (4)$$

where $T$ is force and $\Delta L$ is displacement from the rest position.

The decoupling spring proposed here suggests that some of the instantaneous compliance attributed above to the series elastic element in the passive muscle is shared with the additional spring, so that the series spring in the passive muscle is slightly stiffer than indicated. To the extent that

TABLE II
CONSTANTS DESCRIBING COMPONENTS IN THE MODEL

| Component | Constant | Symbol | Value | Units |
|---|---|---|---|---|
| Springs | | | | |
| Series | Length constant | $k_s$ | 0.02 | $L_{max}$ |
| | Force asymptote | $To_s$ | 0.01 | $mN$ |
| Parallel | Length constant | $k_p$ | 0.05 | $L_{max}$ |
| | Force asymptote | $To_p$ | 0.01 | $mN$ |
| Decoupling | Spring constant | $h$ | 616 | $mN/L_{max}$ |
| Dashpots | | | | |
| Series | Damping Constant | $Q_s$ | 0.15 | $mN \cdot s/L_{max}$ |
| Parallel | Damping Constant | $Q_p$ | 39 | $mN \cdot s/L_{max}$ |

Values for muscle 2 used in figures calculating the responses in Figs. 5 and 6.

this is so, the series spring in the passive muscle will not fully account for all the series elastic recoil in the active muscle. Such a discrepancy is to be expected, however, because a small amount of the total compliance in the active muscle is in the cross-bridges of the contractile elements.

## Calculated Responses

To determine whether the model proposed for the passive muscle will account for the behavior of the active muscle, the responses of both length and force steps applied to the model in Fig. 2 *E* were calculated using the numerical procedure described in the Appendix. First, the force responses of the passive muscle to length ramps were calculated. The light damping of the series spring (by dashpot *s*) was defined by the constant, $Q$, in Eq. 3, and its magnitude was estimated by matching the force steps at the beginning and end of the ramps applied to the passive muscle (stages 1 and 3, Fig. 1 [*inset*]). The value of $h$ in Eq. 4, the slope of the linear extension-force relation of the decoupling spring, was obtained by matching the rounding of the force steps at the end of the ramps (stage 3). Calculated force responses to length changes applied to the passive muscle are shown as the third trace in each of the panels of Fig. 5. The constants used for these calculations are listed in Table II. The fourth trace is the difference between the calculated and observed force, amplified 2.5 times. As shown, there is a fairly good agreement between the calculated and observed records. The disagreement between the calculated values and the data at the end of the ramp in the lowest panels is attributed to the muscle going slack. Most of the rapid recovery following a ramp is complete within 1 ms, but a small amount of rapid recovery takes 4–5 ms to complete, and is shown as an upward deviation of the difference traces in Fig. 5. This slower process can be explained by inhomogeneities in the damped series element, and is described in greater detail below. There is also a small disagreement at the beginning and end of the ramp, the major part of which is probably due to the inertia of the muscle.[2]

The values for the series elastic and viscous elements obtained in the passive muscle were used to calculate the shortening associated with a force step applied to the active muscle, using the recorded force step as a driving function. In this way, the series elements could be evaluated with respect to both compliance and damping. The velocity records rather than the length records are compared because rounding of the isotonic length records following large force steps made it difficult to estimate the extent of series elastic recoil. A set of comparisons between calculated and observed velocity records is shown in Fig. 6. Three force steps were made at each of two lengths and three different times in the twitch, so that records from eighteen separate contractions are shown. The three times in the twitch were during the rise of force, at the peak of force, and during relaxation, representing different contractile states. The two lengths were chosen so that the correction for rest force would be substantial at the long length and negligible at the short length. The bottom set of three traces in each panel shows the difference between the observed and calculated response at a 2.5 times greater gain. Integration of the difference yields the amount of muscle shortening not accounted for by the model, which amounted to 10–20% of the total series elastic recoil. This residual difference is attributed to contractile element shortening. Many of the difference traces have properties similar to the velocity transients described in skeletal muscle (Podolsky, 1960; Civan and Podolsky, 1966; Huxley and Simmons, 1972). There is an immediate rapid

[2]Some rapid force changes are expected to result from the inertia of the fiber and the resonance of the transducer (Ford et al., 1977). The observation that the entire force ramp (stage 2, Fig. 1) lies below, and approximately parallel to an imaginary line joining the force records at the beginning and end of the ramp suggests that most of the rapid force response is due to the length change being applied directly to a viscous element. Force responses due to inertia, either of the fiber or the transducer, would be expected to approach this imaginary line.

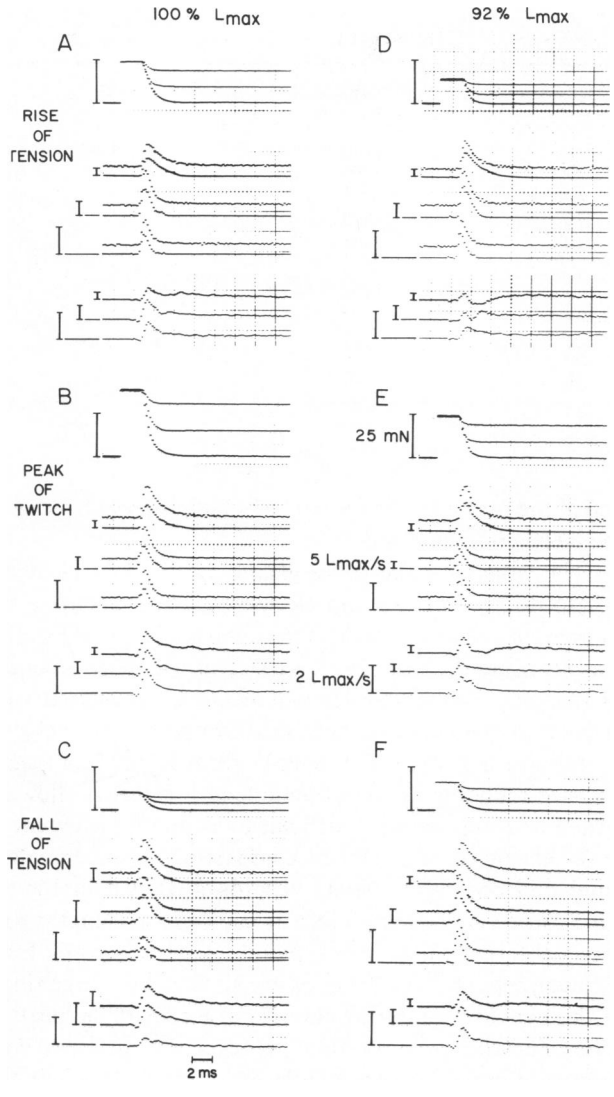


FIGURE 6 Damped series elastic recoil velocity. Three force steps applied at each of three times after stimulation, two different lengths. *A*, 200 ms, 100% $L_{max}$. *B*, 400 ms 100% $L_{max}$ (same steps as in Fig. 4). *C*, 700 ms 100% $L_{max}$. *D*, 200 ms, 92% $L_{max}$. *E*, 400 ms, 92% $L_{max}$. *F*, 800 ms, 92% $L_{max}$. Upper traces in each panel, the three force steps superimposed. Middle traces, the three velocity records paired with the calculated damped series elastic recoil. The lower record in each pair is the calculated recoil. The lower traces in each panel are the differences between the two on a 2 1/2 times greater scale. These difference traces have been digitally filtered, which accounts for the negative deflection at the onset of the step. The velocity gains are increased for the steps to higher force, with the calibration bars all having the same value.

shortening following the step, followed by a decline of velocity and then acceleration to the isotonic level. Fig. 6 also shows that the damped series elastic recoil ends by 5–10 ms after the onset of the step.

## Distributed Series Compliance

Fig. 5 shows a slight mismatch between the calculated and observed force responses immediately following ramps applied to the passive muscle. As mentioned above, the fit could be improved by assuming that the series dashpot and spring were distributed into several components. To test this hypothesis, the series elements in Fig. 2 *E* were divided into two damped springs of equal compliance and damping factors that were different by a factor of 6 (Fig. 2 *F*). Such a division might be envisioned physically as representing the compliance at the two ends of the muscle, with the tendon end having less damping than the crushed tissue at the other end. The total compliance of these two elements was equal to that of the single element used in calculating the records shown in Fig. 5. The response to a rapid length ramp applied to the passive muscle was calculated using an extension of the method described in the Appendix. As shown in Fig. 7 *A*, there is better agreement than when a single, lumped series element is used.

Because one of the main purposes of this analysis was to assess the contribution of damped series element recoil to the measured velocity, the recoil velocity of the distributed series compliance was also calculated. The case of the largest force step in Fig. 4 is shown in Fig. 7 *B*. As

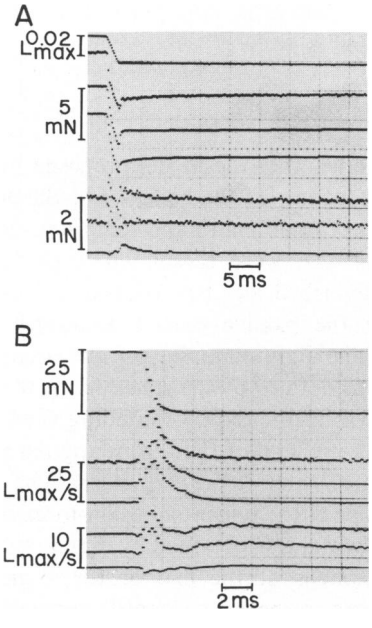


FIGURE 7 Effect of distributed series compliance. *A*, Length steps applied to passive muscle. Same step as middle panel in Fig. 5. Top trace, the length step. Second trace, the measured force response. Third trace, force response calculated on the basis of compliance lumped into a single element. Fourth trace, force response calculated on the basis of the same compliance distributed between two elements having equal compliance and damping factors different by a factor of 6. Fifth trace, difference between real response and response calculated as the basis of a lumped compliance. Sixth trace, difference between real response and response calculated for a distributed compliance. Bottom trace, difference between the two calculated responses. *B*, Force step applied to the active muscle. Same step as the largest step in Fig. 7 *E*. Top trace, force. Second trace, measured velocity. Third trace, recoil velocity of the lumped element. Fourth trace, recoil velocity of the distributed element. Fifth trace, difference between the measured velocity and the recoil of the lumped series element. Sixth trace, difference between the measured velocity and the recoil of the distributed compliance. Bottom trace, difference between the two calculated recoil velocities. All the difference traces are displayed at 2 1/2 times the gain of the responses.

illustrated, the difference between the responses of the lumped and distributed elements is very small, and confined mainly to the very early response. In both cases, the velocity of the series element is zero by 7–8 ms after the onset of the step.

*Magnitude of Series Elastic Extension.* A major problem with the study of cardiac muscle is that the compliant series spring allows the contractile elements to shorten substantially during the development of isometric force. Observations made at the peak of the twitch are therefore appropriate to a much shorter sarcomere length than those made early in the twitch. The nonlinear nature of the series spring described here suggests that it would be stretched enormously (>15% $L_{max}$) if muscle force were to rise from zero to its isometric maximum, because the series element is very compliant near zero force. Very much smaller changes of sarcomere spacing were actually encountered during an isometric twitch. At long lengths, there is a finite rest force, so that force does not begin at zero; at shorter lengths, where there is little rest force, maximum force is not achieved. In the muscles used here, the maximum series elastic extension seen at $L_{max}$ was estimated to be 3–4% $L_{max}$. At shorter lengths, where rest force was lower and the series element more compliant, 5–6% $L_{max}$ extension occurred as isometric force developed. These values agree with microscopic observations of the contracting muscle.

*Localization of the Series Elastic Element.* Carbon granules were placed on the muscles and observed during isometric contractions and releases to zero load. No granules were observed to move by >2% $L_{max}$ during isometric contractions, and the greatest relative movement occurred at the ends of the muscle, where granules could be seen to move away from the edge of the clip. Figs. 8 *A*, *B*, and *C* show 16-mm cine photographs of the muscle at rest, at the peak of force development, and ~25 mm after release to zero load, respectively. Carbon granules at the right-hand end moved away from the clip by ~1.5% $L_{max}$ during isometric force development, and returned to their rest position following the release. There were also transpositions of granules relative to each other in the center of the muscle, indicating internal shear. These findings suggest that most of the series compliance could be accounted for by extracellular tissue, and that much of this was at the ends of the muscle, but the film records lacked sufficient resolution to follow the course of damped elastic recoil at the ends of the muscle.

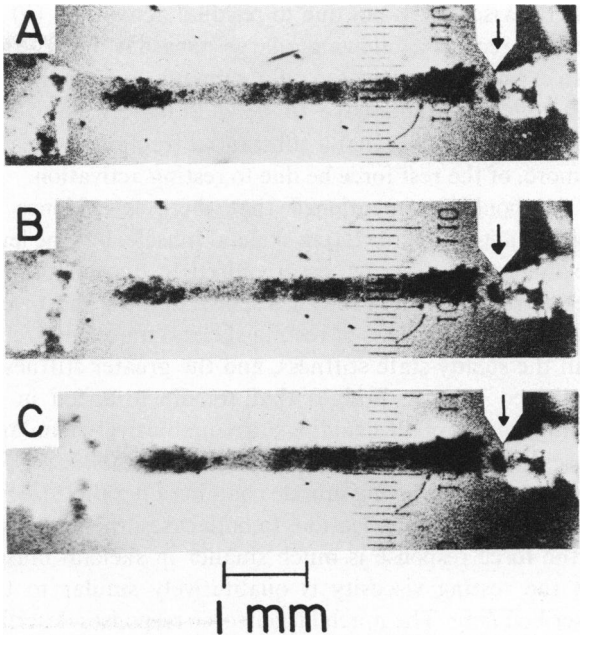


FIGURE 8 Photographs of muscle. *A*, at rest; *B*, at the peak of isometric force; and *C*, ~25 ms after release to near zero force. The arrow at right hand end indicates a carbon granule that has moved relative to the clip by ~1.5% $L_{max}$ during the development of tension and returned to it's rest position following the release.

## DISCUSSION

The main conclusion of this study is that the contractile elements of cardiac muscle are in parallel with a substantial viscous element. "Creep" or stress relaxation suggesting the presence of a viscous element has been described before (Hefner and Bowen, 1967; Little and Wead, 1971; Pinto and Patitucci, 1977) but no previous effort has been made to relate the responsible viscous element to other components. The arrangement described here may help to resolve some of the questions regarding the type of model used to represent cardiac muscle. Hefner and Bowen (1967) found that the instantaneous compliance of the total passive muscle was approximately equal to the series elastic compliance measured in the active muscle, as was found in the present study. They interpreted this finding as strongly supporting the Maxwell configuration. They reasoned that if the springs were arranged in the Voigt configuration, the parallel elasticity would have to be nearly rigid, and therefore could not accommodate extension of the contractile elements. This conclusion is inconsistent with the microscopic observations of Krueger and Pollack (1975), as well as those described here, and with the more recent results from Hefner's laboratory (Donald et al., 1980) showing that a substantial fraction of the series elasticity of the papillary muscle is in its ends, and therefore likely to be in series with all other structures, including those responsible for the parallel elasticity. The present finding that the parallel element is sufficiently damped to be nearly rigid during a step can reconcile Hefner and Bowen's (1967) results with the Voigt model.

*Implications of Parallel Damping.* The conclusion that there is a substantial viscosity in parallel with the contractile elements during diastole raises the question of whether it might be a part of the contractile apparatus, some form of residual activation. Two observations suggest

that the viscosity is not due to residual activation: (*a*) the speed of recovery following a large release is much slower than expected for activated myofilaments, and (*b*) the level of activation would have to be inordinately high. This mechanism requires that a substantial fraction, two-thirds or more, of the rest force be due to resting activation.

It should be mentioned that there is evidence for residual activation in resting skeletal muscle, but the levels are much lower than those required to account for the present results. Hill (1968) has shown that the short range instantaneous stiffness of resting skeletal muscle is greater than the steady-state stiffness, and the greater stiffness is attributed to cross-bridges that remain attached in the resting muscle. Hill's findings are qualitatively similar to those described here. Similarly, Ford et al. (1977, p. 484), have shown that resting muscle contains a parallel viscosity that disappears on activation. In both cases, the magnitude of the force response is much smaller in skeletal muscle, but the resting viscosity is qualitatively similar to that described here. The much larger force responses described here as compared with those in skeletal muscle suggest that the major part of the viscosity is probably due to something other than the contractile apparatus.

Viscosity in parallel with the contractile elements might explain a variable diastolic compliance. In the intact ventricle, viscosity will slow filling and alter the relationship between pre-load and end-diastolic fiber length. Since end-systolic volume varies directly with afterload (Sagawa, 1978), end-diastolic compliance would appear to be greater at higher afterloads if the rate of filling were partially limited by viscosity. Such an inverse relationship between end-diastolic compliance and afterload has been reported by Gilmore et al. (1966) and Janicki and Weber (1977).

## Decoupling Spring

A parallel viscosity of the magnitude measured here will impose a considerable load on the actively shortening muscle. This load would cause a wasteful expenditure of energy if it were coupled rigidly to the contractile elements. The position of the compressive spring in Figs. 2 *E* and *F* is postulated to explain how the working muscle might avoid this energy waste. Such a spring would allow the contractile elements to shorten for some distance before meeting the full resistance of the viscous load. It would also allow some of the energy of contraction to be stored in passive structures and used to hasten diastolic muscle elongation and ventricular filling.

Additional evidence for viscoelasticity in the myocardium comes from several other sources. The following paper shows that such passive viscoelastic resistance to shortening can account for many of the time-dependent changes in the force-velocity characteristics of the activated muscle. Tamiya et al. (1979) found that the rate of isotonic elongation following an afterload twitch in isolated papillary muscle contraction was dependent solely on the distance shortened, and was independent of muscle length or contractile state. A viscoelastic element in parallel with the contractile elements would produce such a result. Pressures below atmospheric are seen in the intact, working ventricle (Brecher, 1958). The muscle must, therefore, contain a compressible compliance that provides a restoring force in early diastole. If this compliance were in series with a viscous element, the restoring force would be independent of initial muscle length. Weiss et al. (1976) have shown that the speed of relaxation of the isolated ventricle is correlated directly with the extent of circumferential fiber shortening, independent of end-systolic fiber length. Their experiments were done on excised hearts that were neurally and hormonally isolated from the remainder of the animal and likely to have been in a constant inotropic state. They concluded that their findings were most easily explained by a viscoelastic element in parallel with the shortening contractile elements, but hastened to add that, at the time of their writing, evidence for such a viscoelasticity in muscle was lacking.

## Series Elements

The measured damping of the series element was so small that it prolonged the recoil by only a few milliseconds. This light damping might be expected to occur, because most of the series compliance resides in the crushed tissue at the ends of the muscle. It has not been reported previously, probably because its observation requires a degree of time resolution not formerly available. An exact comparison of the properties of the series elements in experiments from different laboratories is probably impossible because of the wide variation in the methods of gripping the tissue.

The finding that the extension-force characteristics of the series elements were identical in the active and passive muscle was somewhat unsatisfactory because a small amount of the series compliances measured in the active muscle would be expected to be in the cross-bridges of the contractile elements. The total compliance in the active muscle should be somewhat greater than the series compliance in the passive muscle. This contradiction was resolved by postulating that some of the apparent series compliance in the passive muscle was in the decoupling spring of the parallel viscoelastic element. The compliance of this decoupling spring is not much greater than the total sarcomere compliance measured in isometric skeletal muscle, (Huxley and Simmons, 1971; Ford et al., 1977). It seems unlikely that >15–30% of the series elastic recoil seen here is due to contractile element shortening, however, because the extent of shortening associated with the recoil is three to six times larger than the sarcomere compliance measured in skeletal muscle (Ford et al., 1981).

## Description and Location of Elements in the Model

The functions used to describe the elements in the model were the simplest that could be used. Exponential functions

were used to describe extensible springs, both because they have given good descriptions of the stress-strain characteristics of the series elasticity in papillary muscles in the past (Parmley and Sonnenblick, 1967; Forman et al., 1972) and because they can give a reasonably good description of the curved functions using only two constants. The quality of the fitted traces indicates that those choices were reasonable.

It seems likely that most of the series compliance in the muscle resides in the crushed tissue at the ends, although the observation of shear along the muscle suggests some additional compliance in the cell-to-cell connections. Eq. 3 seems a reasonable description of the damping in these elements, inasmuch as the damping results from fluid moving through the interstices of the connective tissue and would resemble a simple dashpot. The nature of the parallel springs and dashpot is less well understood. If this parallel viscosity is a useful adaptation that aids ventricular filling, it would be reasonable to suppose that it is due to a well-organized structure, which would not be found in skeletal muscle, where such a viscoelasticity would provide no functional benefit. The further possibility must be considered that the viscosity is due to a plastic structure which changes shape as the result of the formation and breaking of chemical bonds, in which case Eq. 3 would only be an approximate description of its behavior.

## APPENDIX

Length and force changes in the muscle were calculated using the model in Fig. 2 *E*. Eq. 2 in the text was used to describe the extension-force characteristics of the two springs in parallel with the viscous elements, the subscripts s and p are used to identify them either as the series or parallel spring. The subscript d denotes the decoupling spring that is in series with the parallel viscosity, Eq. 4. The force-velocity relationship of the two viscous elements are described by Eq. 3, again with the subscripts s and p to distinguish them.

*Series Elastic Recoil.* The overall force on the muscle ($T$) equals the force on the entire series element which in turn is the sum of the forces on the series spring and the dashpot in parallel, so that

$$T = [(T_{os} + T_{is})\, e^{\Delta L_s/k_s} - T_{os}] + \left[Q_s \frac{d\Delta L_s}{dt}\right] \quad \text{(A1)}$$

or

$$\frac{d\Delta L_s}{dt} = [T + T_{os} - (T_{os} + T_{is})\, e^{\Delta L_s/k_s}]/Q_s \quad \text{(A2)}$$

where $\Delta L_s = L_s - L_{is}$. $L_{is}$ and $T_{is}$ are the initial SE length and force just before the quick release. $T_{is}$ is also equal to $T_i$, the initial muscle force. During the force step, Eq. A2 cannot be solved analytically because $T$ is arbitrarily determined by the step, so a fourth-order Runge-Kutta algorithm (Carnahan et al., 1969, p. 361) was used to evaluate $\Delta L_s$ numerically with the initial condition being $\Delta L_{is} = 0$. $\Delta L_s$ was then differentiated to give $V_s$, the recoil velocity. When the force step was 98% complete it was assumed to have attained its final value, i.e., $T$ is constant thereafter. This allows Eq. A2 to be solved exactly for $V_s$ by direct integration:

$$V_s = \frac{(T + T_{os})/Q_s}{1 + \dfrac{(T_i + T_{os})}{V'_s \cdot Q_s}\, e^{\Delta L'_s/k_s}\, e^{(T+T_{os})t/(k_s \cdot Q_s)}} \quad \text{(A3)}$$

where $V'_s$ is the SE velocity and $\Delta L'_s$ the total SE length change at the point when the force step just reached its final value; both were given by the Runge-Kutta method above. This is the point of switching over from solving Eq. A2 by numerical method to direct solution.

*Force Response to a Length Ramp-Applied to the Passive Muscle.* Because the SE and PE are in series, (Fig. 2 *E*) the force across them is the same and equal to the muscle force ($T$). The series component force is made up of the series spring and viscous element force as in Eq. A2 above. The parallel component force is the sum of the force in the parallel spring, the force in the contractile element that is zero and the force in the linear decoupling spring (spring *d*) and dashpot arrangement whose combined instantaneous force-extension relationship is described by

$$dL_p/dt = T_d/Q_p + 1/h \cdot dT_d/dt. \quad \text{(A4)}$$

The parallel element length is equal to the total muscle length ($L$) minus the series element length

$$L_p = L - L_s \quad \text{(A5)}$$

or

$$\Delta L_p = \Delta L - \Delta L_s. \quad \text{(A6)}$$

The force in the decoupling spring and dashpot is given by the muscle force minus the parallel spring force so that

$$T_d = T - T_p. \quad \text{(A7)}$$

Substituting Eq. A1 for $T$ and the spring equation (Eq. 2 in text) for $T_p$ into Eq. A7 gives an expression for $T_d$ in terms of $\Delta L_s$ and $\Delta L_p$, but $\Delta L_p$ can be expressed in terms of $\Delta L_s$ (Eq. A6) so that

$$T_d = \left[A - T_{os} + Q_s \frac{d\Delta L_s}{dt}\right] - [B - T_{op}] \quad \text{(A8)}$$

where

$$A = (T_{os} + T_{is})\, e^{\Delta L_s/k_s}$$

and

$$B = (T_{op} + T_{ip})\, e^{(\Delta L - \Delta L_s)/k_p}$$

substituting Eq. A8 and the derivatives of Eqs. A5 and A8 into A4 yields a second-order differential equation in $\Delta L_s$

$$\frac{d^2\Delta L_s}{dt^2}\left(\frac{Q_s}{h}\right) + \frac{d\Delta L_s}{dt}\left(\frac{Q_s}{Q_p} + \frac{A}{h \cdot k_s} + \frac{B}{h \cdot k_p} + 1\right) + \frac{1}{Q_p}[A - T_{os} - B + T_{op}] - \frac{d\Delta L}{dt}\left[\frac{B}{h \cdot k_p} + 1\right] = 0. \quad \text{(A9)}$$

This can be reduced to two simultaneous first order differential equations by substituting $Y$ for $(d\Delta L_s)/(dt)$ in Eq. A9

$$\frac{d\Delta L_s}{dt} = Y \quad \text{(A10)}$$

and

$$\frac{dY}{dt} = -Y\left[\frac{1}{Q_s}(A/k_s + B/k_p) + h\left(\frac{1}{Q_s} + \frac{1}{Q_p}\right)\right]$$
$$- \frac{h}{Q_s}\left\{\frac{1}{Q_p}[(A - B) - (T_{os} - T_{op})] - \frac{d\Delta L}{dt}\left(\frac{B}{h \cdot k_p} + 1\right)\right\} \quad (A11)$$

These two equations can be solved simultaneously using the fourth-order Runge-Kutta method. The initial conditions are $\Delta L_s = 0$, $Y = (d\Delta L_s)/(dt) = 0$, and $T_{ip} = T_{is} = T_i$ = muscle force before the ramp. $(d\Delta L)/(dt)$ is the slope of the length ramp and is equal to zero after it ends. Finally, by substituting the values of $\Delta L_s$ and $(d\Delta L_s)/(dt)$ calculated above into Eq. A1, the total muscle force could be obtained.

We thank Mr. Jules Quinlan for technical help and Drs. Alan J. Brady and Richard D. Coulson for comments on the manuscript.

Dr. Ford was an Established Investigator of the American Heart Association. Dr. Ballou was a Post-doctoral Fellow of the Chicago Heart Association. The work was supported by United States Public Health Service grant HL-20592 and a grant from the American Heart Association.

*Received for publication 21 May 1981 and in revised form 10 November 1981.*

## REFERENCES

Abbott, B. C., and W. F. H. M. Mommaerts. 1959. A study of inotropic mechanisms in the papillary muscle preparation. *J. Gen. Physiol.* 42:533–551.

Brecher, G. A. 1958. Critical review of recent work on ventricular diastolic suction. *Circ. Res.* 6:554–566.

Carnahan, B., H. A. Luther, and J. O. Wilkes. 1969. Applied Numerical Methods. John Wiley & Sons, Inc., New York. 1–604.

Chiu, Y.-L., S. Karwash, and L. E. Ford. 1978. A piezo electric force transducer for single muscle cells. *Am. J. Physiol.* 235:C143–146.

Civan, M. M., and R. J. Podolsky. 1966. Contraction kinetics of striated muscle fibres following quick changes in load. *J. Physiol. (Lond.).* 184:511–534.

Donald, T. C., D. N. S. Reeves, R. C. Reeves, A. A. Walker, and L. L. Hefner. 1980. Effect of damaged ends in papillary muscle preparations. *Am. J. Physiol.* 238:H14–H23.

Forman, R., L. E. Ford, and E. H. Sonnenblick. 1972. Effect of muscle length on the force-velocity relationship of tetanized cardiac muscle. *Circ. Res.* 31:195–206.

Ford, L. E., A. F. Huxley, and R. M. Simmons. 1977. Tension responses to sudden length change in stimulated frog muscle fibres near slack length. *J. Physiol. (Lond.).* 269:441–515.

Ford, L. E., A. F. Huxley, and R. M. Simmons. 1981. The relation between stiffness and filament overlap in stimulated frog muscle fibers. *J. Physiol. (Lond.).* 311:219–249.

Gilmore, J. P., H. E. Cingolani, R. R. Taylor, and R. H. McDonald, Jr. 1966. Physical factors and cardiac adaption. *Am. J. Physiol.* 211:1219–1226.

Gordon, A. M., A. F. Huxley, and F. J. Julian. 1966. Tension development in highly stretched vertebrate muscle fibres. *J. Physiol. (Lond.).* 184:143–169.

Hefner, L. L., and T. E. Bowen, Jr. 1967. Elastic components of cat papillary muscle. *Am. J. Physiol.* 212:1221–1227.

Hill, D. K. 1968. Tension due to interaction between the sliding filaments in resting striated muscle. The effect of stimulation. *J. Physiol. (Lond.).* 199:637–684.

Huxley, A. F., and R. M. Simmons. 1971. Proposed mechanism of force generation in striated muscle. *Nature (Lond.).* 233:533–538.

Huxley, A. F., and R. M. Simmons. 1972. Mechanical transients and the origin of muscular force. *Cold Spring Harbor Symp. Quant. Biol.* 37:669–680.

Janicki, J. S., and K. T. Weber. 1977. Ejection pressure and the diastolic left ventricular pressure-volume relation. *Am. J. Physiol.* 232:H545–H552.

Kendall, M. G. 1976. Time Series. 2nd edition. C. Griffin & Co. Ltd., London. 1–197.

Krueger, J. W., and G. H. Pollack. 1975. Myocardial sarcomere dynamics during isometric contraction. *J. Physiol. (Lond.).* 251:627–643.

Little, R. C., and W. B. Wead. 1971. Diastolic viscoelastic properties of active and quiescent cardiac muscle. *Am. J. Physiol.* 221:1120–1125.

Nakajima, S., A. Gilai, and D. Dingeman. 1976. Dye absorption changes in single muscle fibers: an application of an automatic balancing circuit. *Pflügers Arch. Eur. J. Physiol.* 362:285–287.

Parmley, W. W., and E. H. Sonnenblick. 1967. Series elasticity in heart muscle: its relation to contractile element velocity and proposed muscle models. *Circ. Res.* 20:112–123.

Pinto, J. G., and P. J. Patitucci. 1977. Creep in cardiac muscle. *Am. J. Physiol.* 232:H553–563.

Podolsky, R. J. 1960. Kinetics of muscular contraction: the approach to the steady state. *Nature (Lond.).* 188:666–668.

Pollack, G. H. 1970. Maximum velocity as an index of contractility in cardiac muscle. *Circ. Res.* 26:111–127.

Sagawa, K. 1978. The ventricular pressure-volume diagram revisited. *Circ. Res.* 43:677–687.

Tamiya, K., M. Sugawara, and Y. Sakurai. 1979. Maximum lengthening velocity during isotonic relaxation at preload in canine papillary muscle. *Am. J. Physiol.* 237:H83–H89.

Weiss, J. L., J. W. Frederiksen, and M. L. Weisfeldt. 1976. Hemodynamic determinants of the time-course of fall in canine left ventricular pressure. *J. Clin. Invest.* 58:751–760.